JGR Atmospheres

RESEARCH ARTICLE
10.1029/2018JD029907

Intracloud Lightning Flashes Initiated at High Altitudes and Dominated by Downward Positive Leaders

Ting Wu[1], **Daohong Wang**[1], **and Nobuyuki Takagi**[1]

[1]Department of Electrical, Electronic and Computer Engineering, Gifu University, Gifu, Japan

Key Points:
- A type of special IC flash initiated at high altitudes (>12 km) called "downward +IC flash" is reported for the first time
- Downward +IC flashes are dominated by downward positive leaders
- Downward +IC flashes are produced in thunderstorms with deep convective updrafts (cloud tops higher than 14 km)

Supporting Information:
- Supporting Information S1

Correspondence to:
T. Wu,
tingwu@gifu-u.ac.jp

Citation:
Wu, T., Wang, D., & Takagi, N. (2019). Intracloud lightning flashes initiated at high altitudes and dominated by downward positive leaders. *Journal of Geophysical Research: Atmospheres*, *124*. https://doi.org/10.1029/2018JD029907

Received 29 OCT 2018
Accepted 2 JUN 2019
Accepted article online 17 JUN 2019

Abstract Intracloud (IC) lightning flashes are normally initiated below 10 km and start with upward negative leaders. In this paper, we report a special type of IC flash called "downward positive IC (+IC) flash" which is initiated at high altitudes (mainly above 12 km) and whose initial negative leaders do not propagate upward. Three-dimensional location results of three downward +IC flashes are described in detail. It is demonstrated that downward +IC flashes start with positive leaders propagating downward with speeds on the order of 10^4 m/s and negative leaders propagating horizontally for only a short distance. Downward +IC flashes are produced in thunderstorms with deep convective updrafts (radar echoes of cloud tops typically higher than 14 km). The charge structure responsible for downward +IC flashes is inferred to be a positive dipole including a negative charge region at a normal altitude (near the −10 °C isotherm) and an upper positive charge region at a relatively high altitude (usually above the −50 °C isotherm), with downward +IC flashes likely initiated from the upper positive charge region. Further, lightning flashes in a thunderstorm producing a large number of downward +IC flashes are analyzed. Results show that normal IC flashes in this thunderstorm are also initiated at altitudes closer to the upper positive charge region and usually consist of downward positive leaders propagating for longer distances than upward negative leaders. Based on these results, we propose a relationship between the altitude of the upper positive charge region and initiation locations of IC flashes.

Plain Language Summary Intracloud (IC) lightning flashes are normally initiated below 10 km. In this paper, we report a special type of IC flash called the "downward positive IC (+IC) flash" which is initiated at high altitudes (mainly above 12 km). The structure of downward +IC flashes is distinctly different from that of normal IC flashes. Downward +IC flashes are produced in vigorous thunderstorms with cloud tops higher than 14 km. However, downward +IC flashes tend to produce weak radiation in radio frequencies, rendering them difficult to detect. This may be the reason that downward +IC flashes have never been reported before.

1. Introduction

It is believed that the majority of lightning flashes are intracloud (IC) flashes, which occur inside or between thunderclouds and do not contact the ground. Due to the fact that IC flashes cannot be effectively observed by video cameras, they have been mainly studied via their radio emissions (e.g., Krider et al., 1975; Villanueva et al., 1994; Weidman & Krider, 1979). IC flashes have various morphologies (see a review by Rakov & Uman, 2003, chapter 9). The most common morphology is the bilevel structure as first revealed by lightning interferometer observations (Shao & Krehbiel, 1996) and later confirmed by observations with the Lightning Mapping Array (LMA; e.g., Rison et al., 1999; Riousset et al., 2007). It is now clear that normal polarity IC flashes (i.e., positive IC flashes or +IC flashes) with the bilevel structure usually start with initial negative leaders propagating upward with speeds on the order of 10^5 m/s (Behnke et al., 2005; Wu et al., 2015).

Initiation altitudes of most IC flashes imaged by the LMA and some low frequency lightning locating systems are below 10 km (e.g., Behnke et al., 2005; Caicedo et al., 2018; Karunarathna et al., 2017; Lyu et al., 2016; van der Velde & Montanyà, 2013; Yoshida et al., 2014). Calhoun et al. (2013) reported that the majority of lightning flashes in a supercell were initiated near altitudes of 10 to 11 km and noted that such supercell was "unusual" compared to other storms. In fact, other than some special types of lightning discharges that do not comprise clear leader channels, such as narrow bipolar events (NBEs; e.g., Smith et al., 2004; Wu

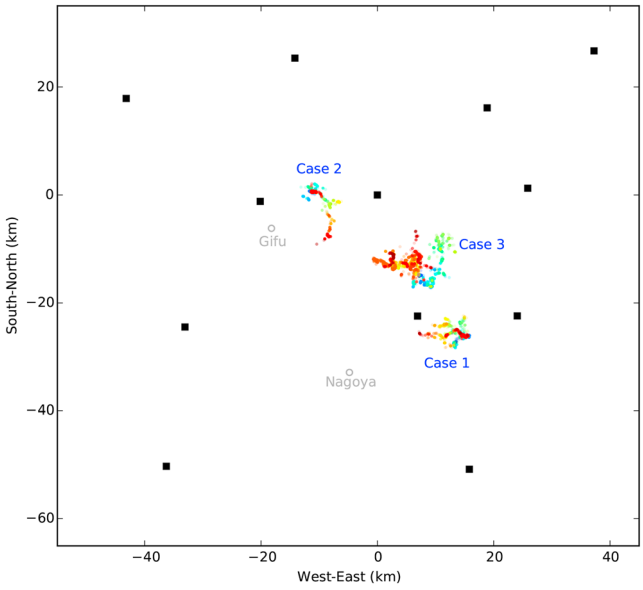

Figure 1. Locations of three flashes analyzed in this paper relative to 12 sites (black squares) of FALMA during the summer of 2017. The origin (0, 0) corresponds to the latitude and longitude of (35.475°E, 136.960°N).

et al., 2012) and discharges in the overshooting tops (e.g., MacGorman et al., 2017), we can find few reports of full-fledged IC flashes initiated at high altitudes such as above 12 km.

On the other hand, according to some statistical distributions of the lightning initiation altitude, there is indeed a small portion of lightning flashes initiated at high altitudes of up to 15 km (Fuchs et al., 2016; Lund et al., 2009; Mecikalski & Carey, 2017). However, development characteristics of these high-altitude flashes and the corresponding charge structures are not clear yet.

In this paper, we will report a special type of IC flash initiated at high altitudes, mainly between 12 and 15 km. We will analyze three cases of these flashes produced in three different thunderstorms and demonstrate that these flashes are fundamentally different from normal IC flashes. They always consist of initial positive leaders propagating downward with speeds on the order of 10^4 m/s. At the same time, however, their initial negative leaders do not propagate upward as in normal IC flashes but propagate horizontally for only a short distance. As will be demonstrated in this paper, these special IC flashes are associated with the same charge structure (the positive dipole) as normal polarity IC flashes, that is, +IC flashes, but their overall development is in a downward direction. Therefore, we will call them "downward +IC flashes."

2. Observation and Data

Data of this study were obtained during the summer of 2017 using the Fast Antenna Lightning Mapping Array (FALMA), a lightning mapping system working in the low frequency band. FALMA can image lightning flashes with great details and high accuracy similar to the LMA. Details of FALMA and examples of lightning flashes imaged by the FALMA can be found in Wu et al. (2018). Twelve sites were set up during the summer of 2017 as shown in Figure 1. Sources of three flashes analyzed in this paper are also plotted in Figure 1. All figures with location information in this paper use the same coordinate as Figure 1.

In all figures showing location results of lightning flashes in this paper, electric field change (E-change) waveforms are also shown. As the magnitude of E-changes has not been calibrated, it is shown in the digital unit. The atmospheric sign convention is used in this paper, so a negative return stroke produces a positive E-change.

In addition, radar data of a nationwide C-band Doppler radar network operated by the Japan Meteorological Agency are used in this study. These data have a spatial resolution of 1 km in both horizontal and vertical directions and a temporal resolution of 10 min. The resolutions are relatively low, so we can only get a general sense of the features of thunderstorms from the radar data. Another problem is that the data only cover altitudes up to 14 km, so cloud top heights of thunderstorms higher than 14 km cannot be determined.

Normal IC flashes start with an upward negative leader and a horizontal or downward positive leader, forming a bilevel structure. The positive leader usually cannot be directly detected but can be inferred from sources of negative recoil leaders. Figure S1 in the supporting information shows an example of a normal IC flash imaged by the FALMA. The initial negative leader first propagated upward and then turned in the horizontal direction. The positive leader mainly propagated horizontally but also had a slightly downward movement. This example demonstrates that FALMA can readily detect recoil leaders and show the development of positive leaders in IC flashes.

The downward +IC flashes reported in this paper are fundamentally different from normal IC flashes, such as that depicted in Figure S1, in that downward +IC flashes start with downward positive leaders but without any upward negative leader.

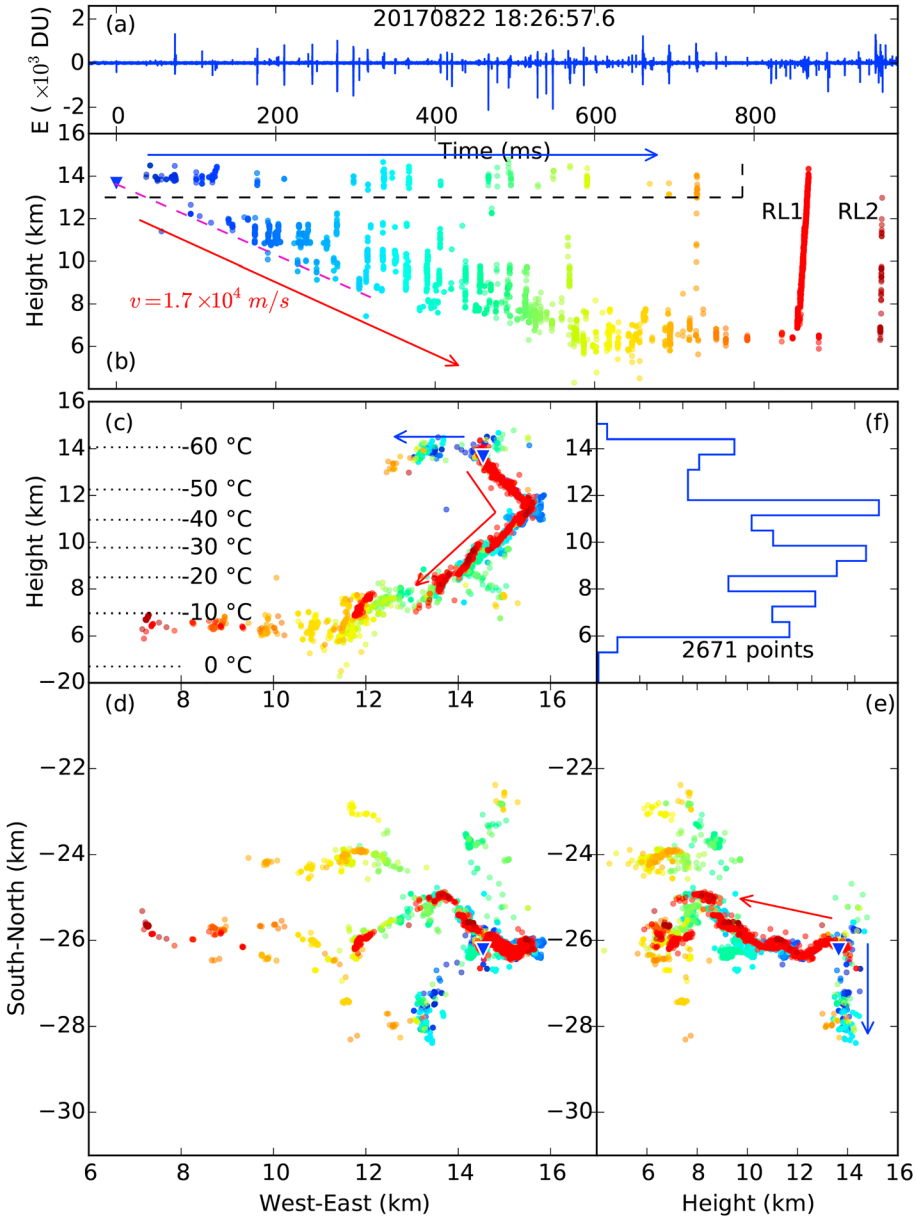

Figure 2. Location results of the first example of a downward +IC flash (Flash One). (a) Electric field change waveform. (b) Height-time view. (c) Height-distance (from west to east) view. (d) Plan view. (e) Distance (from south to north)-height view. (f) Source distribution along the height. The blue triangle represents the first located source of this flash.

3. Results

3.1. Three-Dimensional Structures of Downward +IC Flashes

3.1.1. Flash One

The first example of a downward +IC flash is shown in Figure 2. It had a duration of about 961 ms. The first source of this flash was located at an altitude of 13.6 km, indicated by the blue triangle in Figure 2. From the initiation location, we can see that some sources gradually moved downward as indicated by the red arrow and some sources moved mainly horizontally as indicated by the blue arrow. In the following analysis, we will demonstrate that the downward-moving sources indicate the development of a downward positive leader, and according to the bidirectional leader concept (e.g., Mazur & Ruhnke, 1993), the sources moving in the horizontal direction indicate the development of a negative leader.

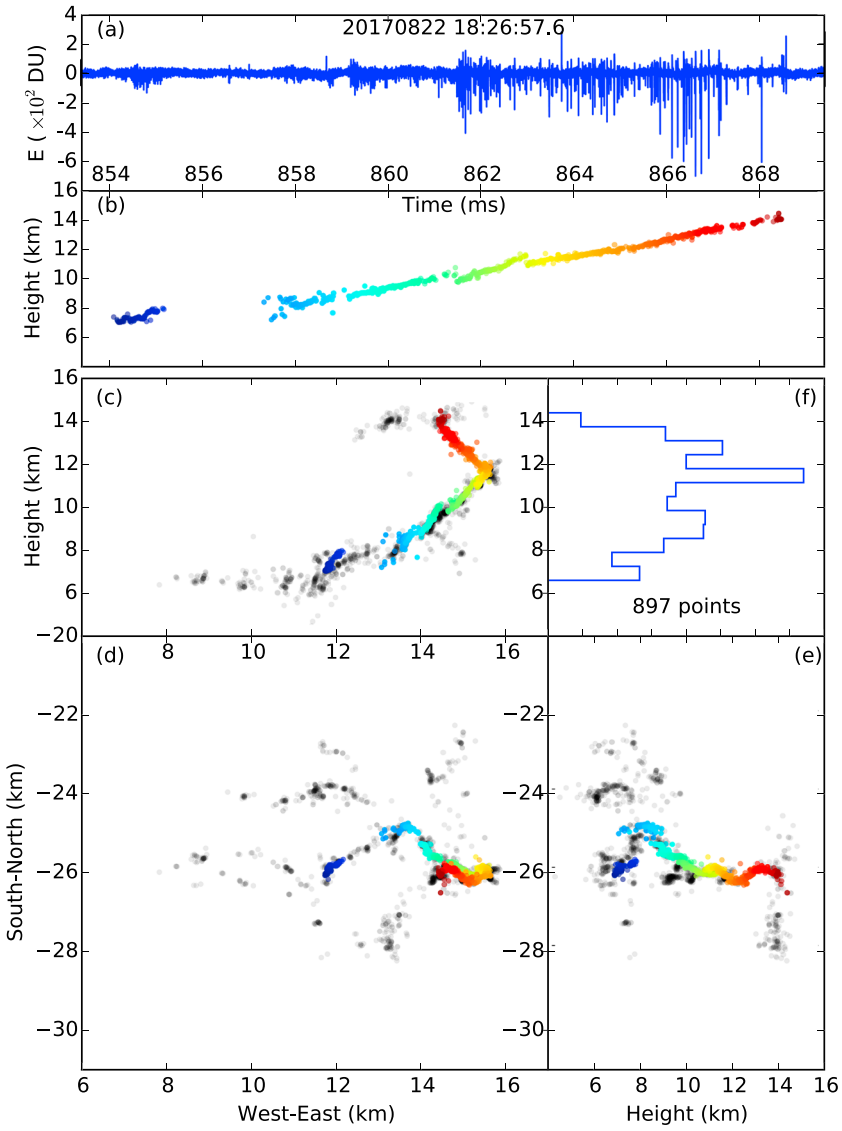

Figure 3. Location results of a recoil leader in Figure 2. Subplots are arranged as in Figure 2. Sources in black are those occurred before the recoil leader.

At the time of about 854 ms, a leader was clearly imaged propagating upward (labeled as RL1 in Figure 2b). Details of this leader are plotted in Figure 3. Sources before this leader are plotted in black. We can see that this leader retraced the old channel and progressed back to the origin of this flash. This leader produced predominantly negative pulses (using the atmospheric sign convention), indicating that it carried negative charges upward. Based on these characteristics, it is clear that this was a negative recoil leader similar to that in normal IC flashes. Accordingly, the old channel it retraced was produced by a positive leader. Note that the speed of this recoil leader was about 5.9×10^5 m/s, which is relatively slow for a recoil leader. It seems that recoil leaders well located by the FALMA are typically those with low speeds. In Figure 2b, we can see that at the end of this flash, these was another recoil leader (labeled as RL2), which retraced the same channel as RL1. The speed of RL2 is estimated to be about 4.9×10^6 m/s, typical for a recoil leader, but only a few sources were located.

Therefore, we conclude that this flash was initiated at an altitude of 13.6 km and started with a downward positive leader and a horizontal negative leader. The downward-moving sources were likely produced by negative recoil leaders retracing the positive leader channel. We can roughly estimate the downward

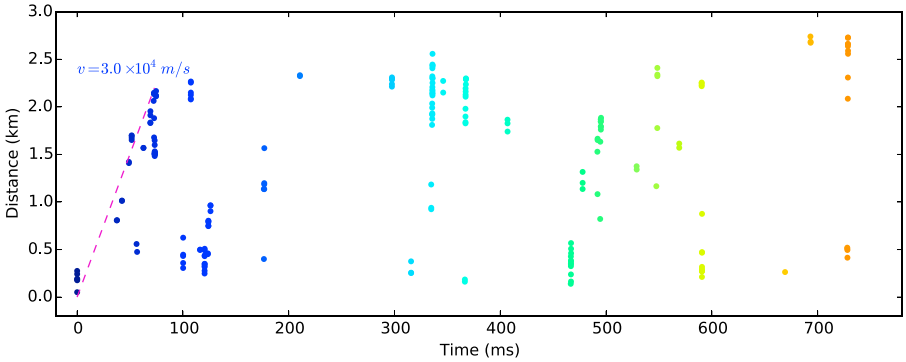

Figure 4. Distance versus time of sources above the black dashed line in Figure 2 (sources of the initial negative leader). Distance is relative to the origin of the flash (the blue triangle in Figure 2). Sources are color coded with the same time scale as those in Figure 2b.

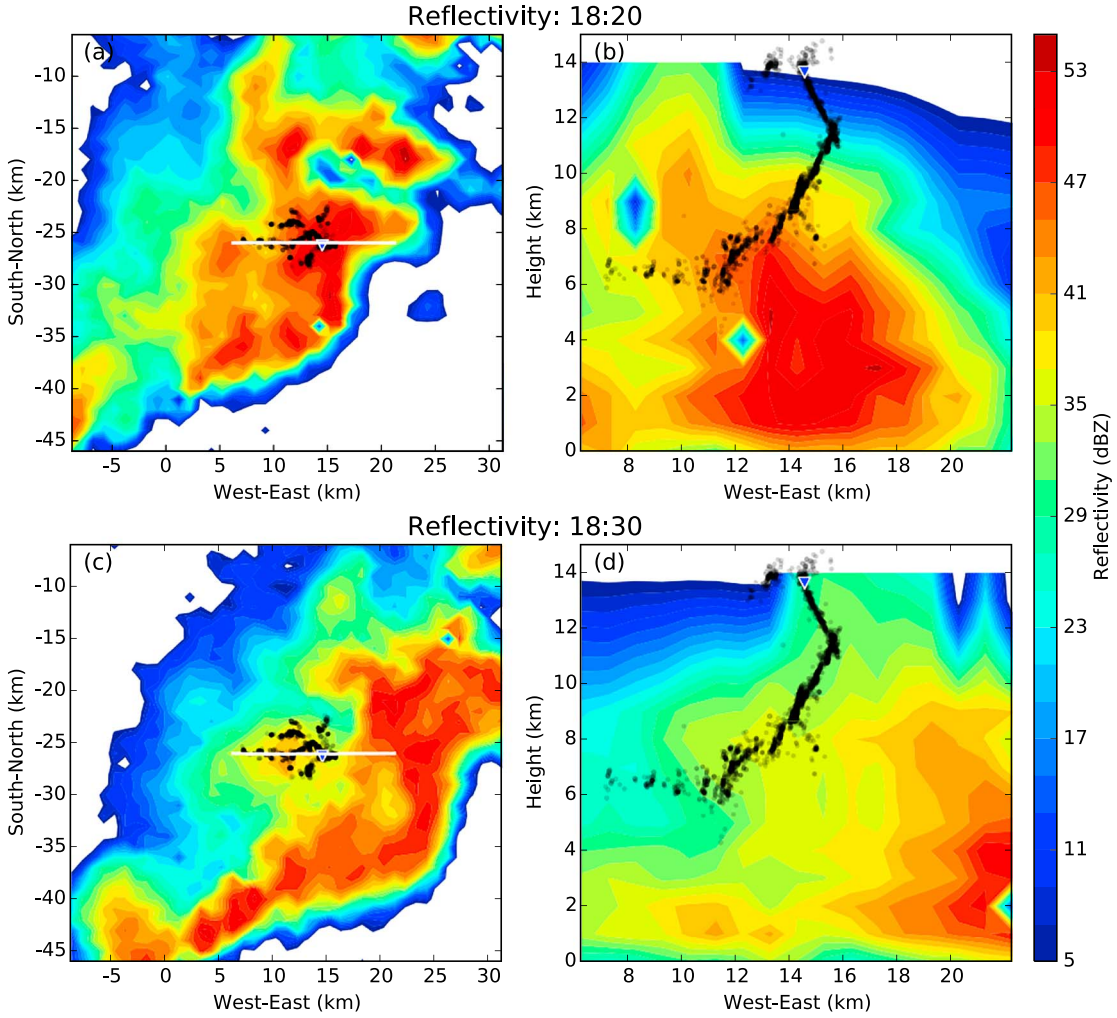

Figure 5. Sources of Flash One superimposed on the radar echo. (a) and (b) show radar reflectivity at the time of 18:20 (about 7 min before the flash). (c) and (d) show radar reflectivity at the time of 18:30 (about 3 min after the flash). (a) and (c) show radar reflectivity at a constant height of 2 km. (b) and (d) show range-height indicator of radar reflectivity at the white lines.

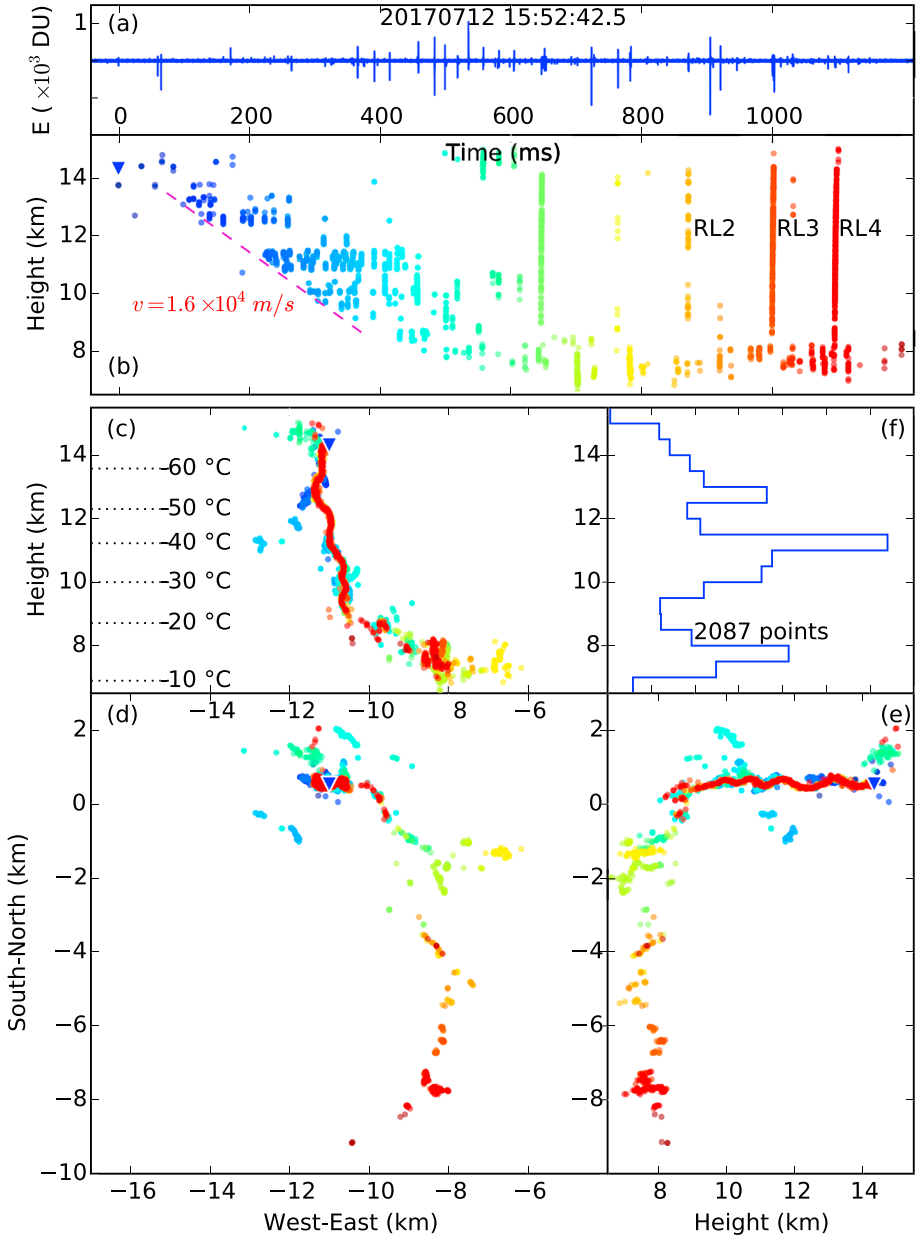

Figure 6. Location results of the second example of a downward +IC flash (Flash Two). Subplots are arranged as in Figure 2. The blue triangle represents the first located source of this flash. RL = recoil leader.

speed of the positive leader from the descending speed of these sources. The speed of the positive leader is estimated to be 1.7×10^4 m/s, represented by the slope of the purple dashed line in Figure 2b.

The initial negative leader, which developed horizontally, apparently had a much lower speed than normal negative leaders. Figure 4 shows the distance-time view of the sources of the negative leader relative to the origin of this flash. Sources above the black dashed line in Figure 2b are selected as those associated with the negative leader. Sources in Figure 4 are color coded with the same time scale as those in Figure 2b. The speed of the negative leader is roughly estimated to be 3.0×10^4 m/s, represented by the slope of the purple dashed line in Figure 4. This value is an order of magnitude smaller than the typical speed of negative stepped leaders. Note that the initial variation of the distance near time zero was due to the random height error of a few sources at the beginning of this flash and was not associated with the

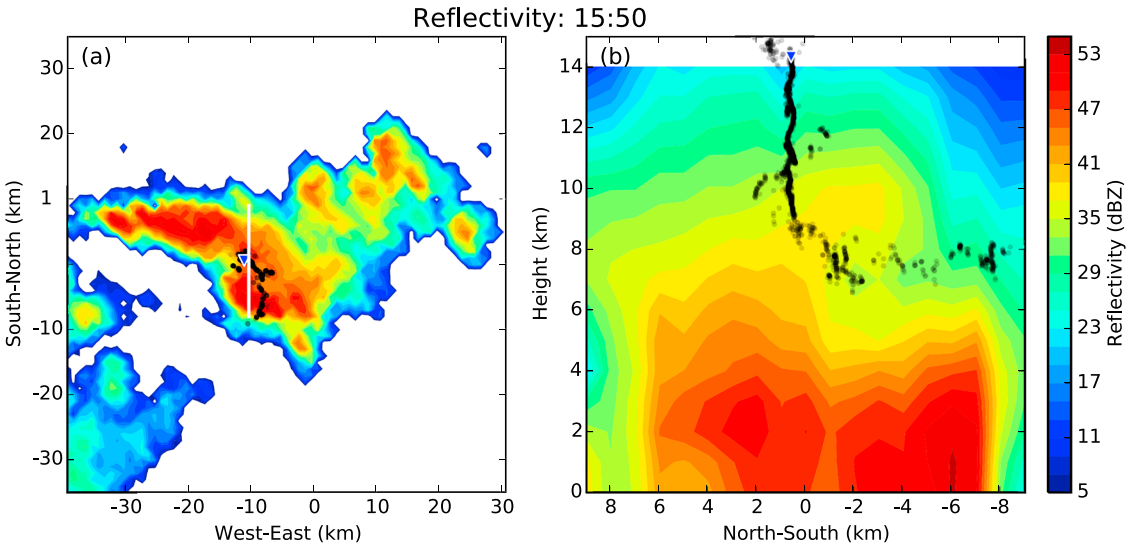

Figure 7. Sources of Flash Two superimposed on the radar echo. (a) Radar reflectivity at a constant height of 2 km. (b) Range-height indicator of the radar reflectivity at the white line.

development of the negative leader. It should also be noted that after the time of about 80 ms, the negative leader had little growth, while the positive leader continued growing. However, it is possible that the sources of the presumed initial negative leader were actually produced by recoil leaders. It seems likely from Figures 2 and 4 that the sources of the initial negative leader did not develop forward spontaneously but was pushed forward by recoil leaders. Currently, we are uncertain of the true physical process of initial negative leaders in downward +IC flashes, but they are apparently different from initial negative leaders in normal IC flashes.

After the time of about 600 ms, the positive leader turned horizontally at the altitude of 6 to 7 km, and several branches can be recognized in the plan view in Figure 2d. The horizontal propagation was likely in a negative charge layer, and it indicates that the negative charge layer was at the altitude of 6 to 7 km. Figure 2c also shows altitudes of 0 to −60 °C isotherms. The isotherm altitudes were obtained by radiosonde observations by the Japan Meteorological Agency at an observation site about 200 km from our observation area, so they were extremely rough estimations. However, we can see that the inferred negative charge layer was close to the −10 °C isotherm, as expected from the noninductive charging mechanism (e.g., Takahashi, 1978). Similarly, the horizontal negative leader can also indicate the positive charge region. It seems that the positive charge region was at an altitude of about 14 km, near the −60 °C isotherm. This is generally higher than the upper positive charge region normally found in thunderstorms (e.g., Stolzenburg & Marshall, 2008).

Figure 5 shows the radar reflectivity of the thunderstorm producing this flash. Figures 5a and 5c show the reflectivity at the altitude of 2 km, and Figures 5b and 5d show the range height indicator (RHI) plot at the white lines in Figures 5a and 5c. As the temporal resolution of the radar data is 10 min, the data before the flash (about 7 min before the flash, Figures 5a and 5b) and after the flash (about 3 min after the flash, Figures 5c and 5d) are both plotted to show the movement of the thunderstorm. We can see that the storm moved in the southeast direction. From the RHI plots (Figures 5b and 5d), we can see that the storm contained a small region of deep convective updrafts extending above 14 km. By comparing Figures 5b and 5d, it seems very likely that the flash was initiated right at the deep convective region. Note that the radar data only cover the altitude below 14 km, so we have no way to know the altitude of the storm top. However, the reflectivity at 14 km altitude in Figures 5b and 5d was larger than 30 dBZ, so it is very likely that this flash occurred inside a very vigorous thunderstorm.

3.1.2. Flash Two

The 3-D location result of the second example is shown in Figure 6. This downward +IC flash had a duration of about 1,198 ms. The first source was located at an altitude of 14.3 km as indicated by the blue triangle in

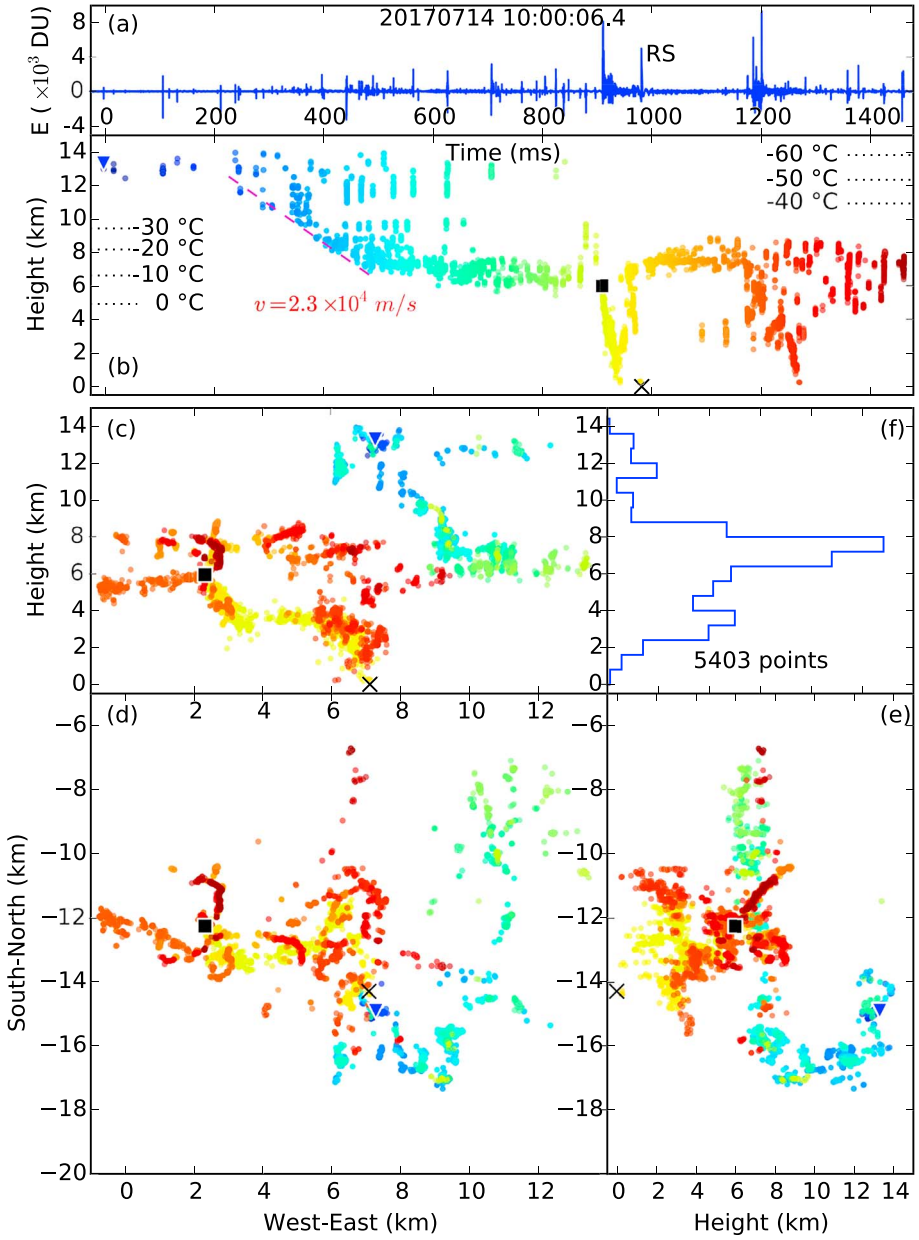

Figure 8. Location results of the third example of a downward +IC flash (Flash Three) along with a −CG flash following it. Subplots are arranged as in Figure 2. The blue triangle represents the first located source of the downward +IC flash. The square represents the first located source of the −CG flash. The cross sign represents a return stroke of the −CG flash. −CG = negative cloud-to-ground.

Figure 6. Note that the sources at the beginning of this flash were scattered, so we are uncertain of the exact initiation altitude of this flash. This seems to be a common problem when locating downward +IC flashes. It seems that pulses at the beginning of downward +IC flashes are especially small and sparse, making it difficult to determine the exact beginning of a flash.

From Figure 6b, we can see that sources gradually moved downward before the time of 600 ms, indicating the downward development of a positive leader similar to that in Flash One. The downward speed of the positive leader is estimated to be 1.6×10^4 m/s, represented by the slope of the purple dashed line in Figure 6b. After the time of about 600 ms, the positive leader mainly developed in the horizontal direction, as can be seen from Figures 6d and 6e. Meanwhile, at least four recoil leaders were well located and are

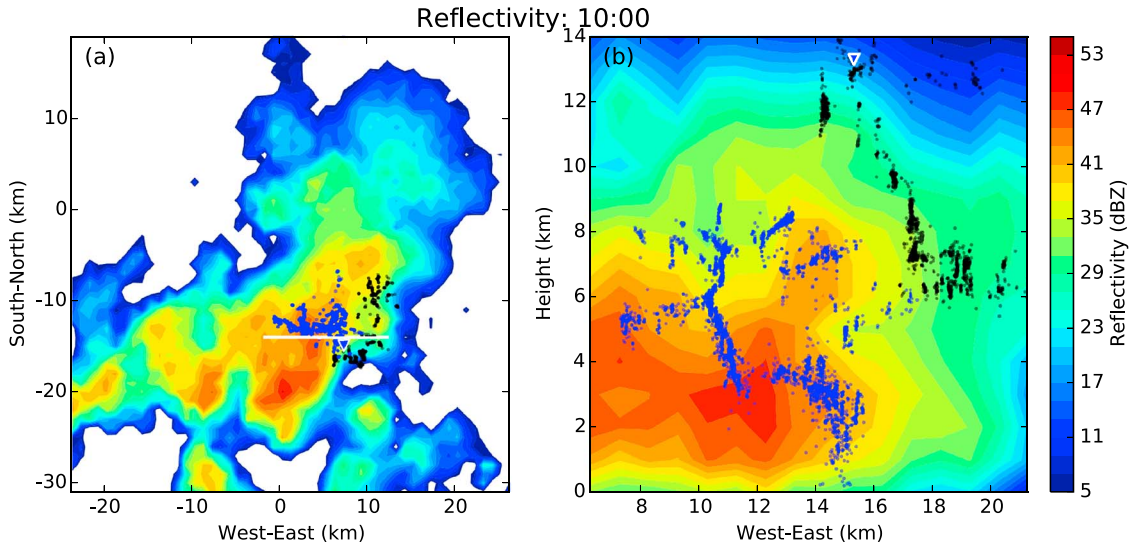

Figure 9. Sources of Flash Three (black) and the subsequent negative cloud-to-ground flash (blue) superimposed on the radar echo. (a) Radar reflectivity at a constant height of 2 km. (b) Range-height indicator of the radar reflectivity at the white line.

labeled as "RL1" to "RL4" in Figure 6b. They were all upward negative recoil leaders. They all traversed the positive leader channel and propagated from the main negative charge region to the origin of this flash. Their estimated vertical speeds are 3.4, 7.3, 2.5, 1.9×10^6 m/s.

The initial negative leader in this flash was not very clear. In Figures 6c and 6e, some sources in green extending outward may indicate the negative leader channel. We did not intend to calculate the speed of the negative leader as only a few sources were detected and the channel was not very clear. However, the speed of the negative leader was apparently much lower than that of the positive leader in this flash.

Figure 6c also shows altitudes of 0 to −60 °C isotherms. Similar to Flash One, the main negative charge layer indicated by the horizontal propagation of the positive leader was near the −10 °C isotherm. If we assume that the positive charge region was near the origin of this flash, it was higher than the −60 °C isotherm. Figure 7 shows sources of this flash superimposed on the radar echo. From the RHI plot in Figure 7b, we can see that this flash was indeed produced in deep updrafts extending above 14 km. The maximum reflectivity at the altitude of 14 km was about 24 dBZ. Similar to the first example, it seems that the charge structure of this thunderstorm included a negative charge layer at a normal altitude (−10 °C isotherm) and a smaller positive charge region at a relatively high altitude (−60 °C isotherm).

3.1.3. Flash Three

In this example, a downward +IC flash was followed by a negative cloud-to-ground (−CG) flash. Location results of the downward +IC flash and the following −CG flash are shown in Figure 8. The downward +IC flash was initiated at an altitude of 13.3 km and lasted for about 899 ms. The −CG flash was initiated about 11 ms after the end of the downward +IC flash. The horizontal distance between initiation locations of these two flashes was about 5.6 km. Examination of Figure 8 reveals that although these two flashes were very near each other, they had no direct contact, and there is no evidence that the −CG flash was initiated by the downward +IC flash. Both of these two flashes indicated a negative charge layer at the altitude of 6 to 8 km, corresponding to the −10 °C isotherm. The occurrence of the −CG flash further confirms that the downward +IC flash consists of a positive leader first going downward and then moving horizontally in the main negative charge layer.

Another special feature of this flash is that, during the first 200 ms, sources were located at almost the same location and did not show any clear development. It seems neither the positive nor negative leaders progressed forward during this period. After about 200 ms, some descending sources were detected, indicating the development of a downward positive leader. The speed of the positive leader is estimated to be 2.3×10^4 m/s represented by the slope of the purple dashed line in Figure 8b. Currently, it is not clear what kind of discharges occurred during the first 200 ms of this flash. As mentioned in section 3.1.2, pulses at the

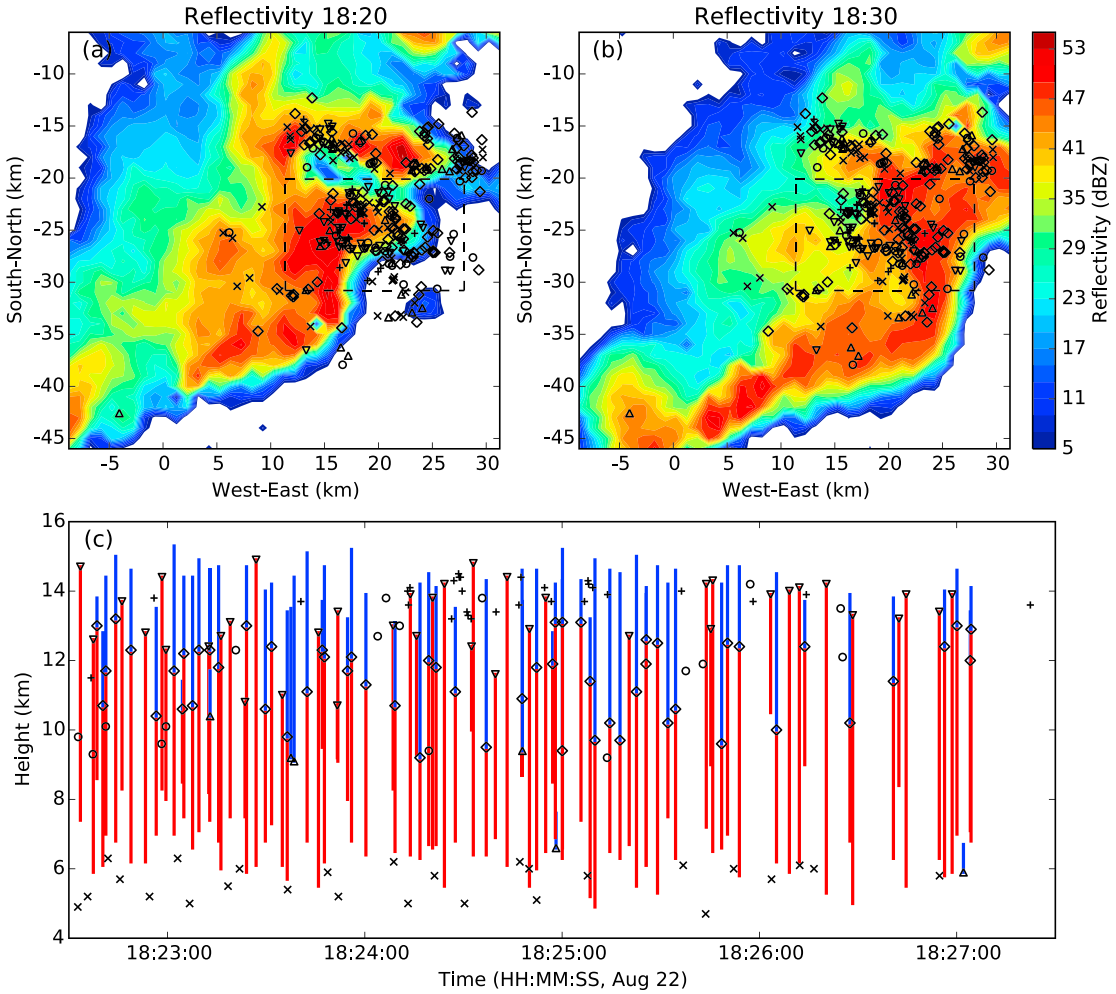

Figure 10. Initiation locations of all lightning flashes during 18:22:30–18:27:30 superimposed on the radar echo. Downward triangles (▽) represent downward +IC flashes. Upward triangles (△) represent IC flashes starting with upward negative leaders. Diamonds (⋄) represent IC flashes starting with both upward negative leaders and downward positive leaders. Cross signs (×) represent negative cloud-to-ground flashes. Plus signs (+) represent isolated positive narrow bipolar events. Circles (○) represent flashes with no clear types. Blue vertical lines represent upward negative leaders, and red vertical lines represent downward positive leaders. Flashes in (c) are those in the dashed boxes in (a) and (b). IC = intracloud.

beginning of downward +IC flashes are especially small and infrequent and are thus difficult to locate. It is possible that the stationary discharges in this example are a common phenomenon for downward +IC flashes but were not well-located in most cases.

The radar echo along with locations of this downward +IC flash and the following −CG flash are shown in Figure 9. The cloud top was higher than 14 km, and the maximum reflectivity at 14 km was about 17 dBZ. Similar to the first two examples, we conclude that Flash Three was also produced inside a thunderstorm with deep convective updrafts.

3.2. Lightning and Storm Characteristics When Downward +IC Flashes Occur

In order to further investigate the charge structure for the production of downward +IC flashes and their relationship with other lightning flashes, we examined lightning flashes in a short period from 18:22:30 to 18:27:30 on 22 August in a thunderstorm with frequent downward +IC flashes. Initiation locations of all lightning flashes during this period are plotted over radar reflectivity at 18:20 and 18:30 as shown in Figures 10a and 10b. Note that the radar reflectivity data in Figures 10a and 10b are the same as those in Figures 5a and 5c. There are 48 downward +IC flashes (represented by "▽"), 120 normal IC flashes starting with both upward negative leaders and downward positive leaders (represented by "⋄"), 26 normal IC

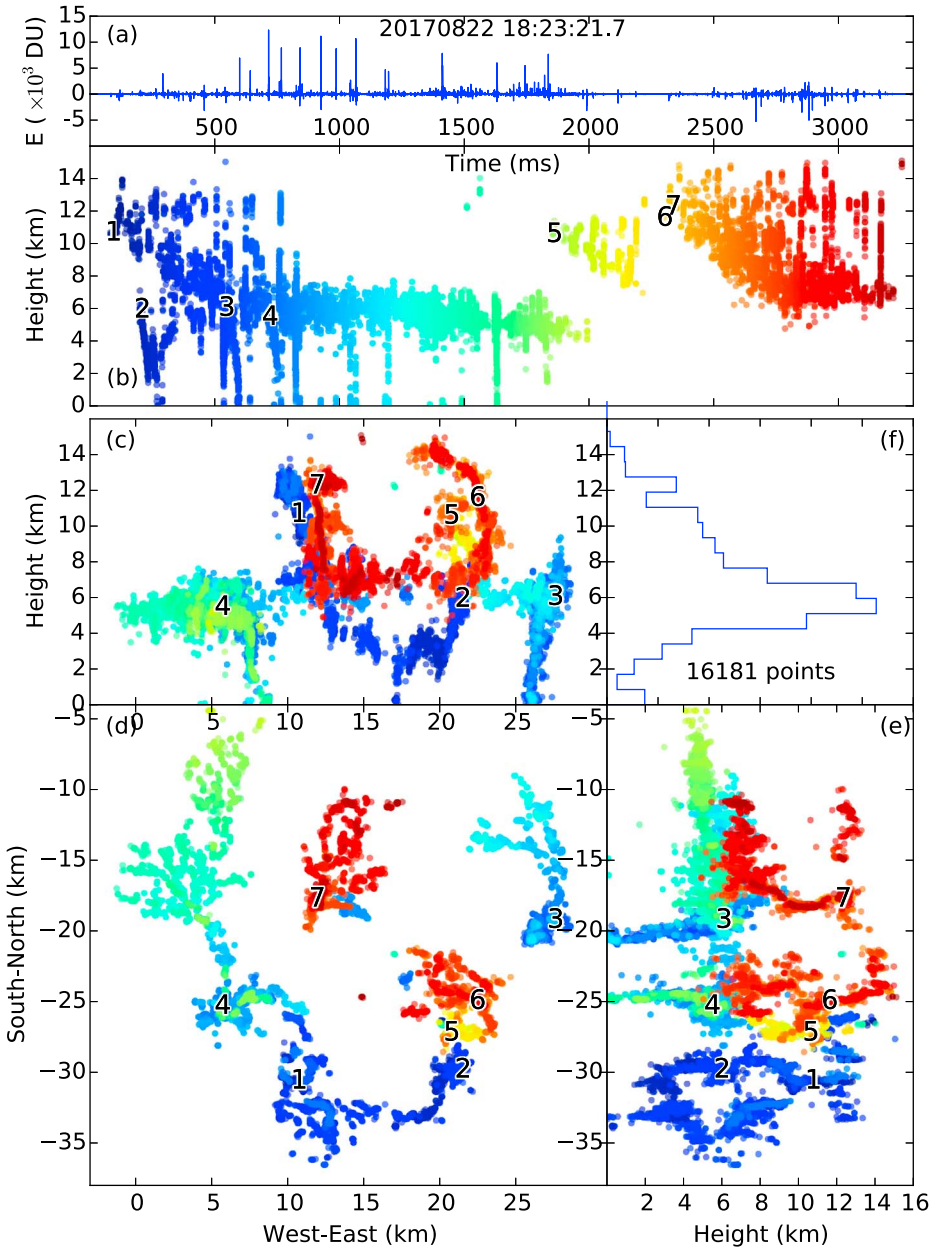

Figure 11. Location results of lightning flashes during about 3 s from 18:23:21.7 in the storm in Figure 10. Subplots are arranged as in Figure 2. At least seven flashes can be identified. Initiation locations of these seven flashes are labeled by numbers. Location results of these seven flashes are shown in Figures S2–S8.

flashes starting with upward negative leaders but without downward positive leaders (represented by "△"), 64 −CG flashes (represented by "×"), 30 isolated positive NBEs (represented by "+"), and 33 flashes with no clear types (represented by "○"). Excluding positive NBEs and flashes with no clear types, a total of 258 flashes occurred during the 5-min period, indicating a relatively high flash rate (e.g., compared to Liu et al., 2012). According to the analysis in section 3.1, it has been clear that downward +IC flashes are produced in thunderstorms with high cloud tops. Therefore, the high flash rate is an expected result considering the theory that the flash rate is correlated with the storm top height (e.g., Ushio et al., 2001).

Location results of lightning flashes during about 3 s from 18:23:21.7 are further shown in Figure 11 for additional details. Close scrutiny of the 3-D structure in Figure 11 reveals that there were at least seven independent flashes, including four −CG flashes, two downward +IC flashes, and two normal IC flashes with both

upward negative and downward positive leaders. Initiation locations of these flashes are labeled by numbers in Figure 11 in accordance with the time sequence. Location results of these seven flashes are shown in Figures S2–S8. Figure 11 illustrates the feature that when downward +IC flashes occur (and when the storm top is very high), multiple lightning flashes can occur simultaneously in different regions of the storm, resulting in a high flash rate. It should also be noted that without detailed location results, it would be extremely difficult to accurately group sources to flashes when multiple flashes occurred within a short period and within a small area, such as the case in Figure 11.

Lightning flashes within dashed boxes in Figures 10a and 10b are further shown in Figure 10c with extensions of upward negative leaders (blue lines) and/or downward positive leaders (red lines). Negative leaders of −CG flashes always moved downward to the ground and are not shown in Figure 10c. From Figure 10c, it is clear that the main negative charge region was at the altitude of about 6 km (corresponding to the temperature of −10 to 0 °C according to Figure 2c) where −CG flashes started. The upper positive charge region was at the altitude of about 15 km but had some variations. Altitudes of positive NBEs were also in agreement with an upper positive charge region at about 15 km (Wu et al., 2012). This result further confirms that a negative charge region at a normal altitude and an elevated upper positive charge region are responsible for the production of downward +IC flashes.

It is also interesting to note that normal IC flashes with only upward negative leaders (such as the example in Figure 3 in Rison et al., 1999) are rare in Figure 10. Most IC flashes started with both upward negative leaders and downward positive leaders, and the downward positive leaders usually extended for a larger distance (red lines are generally longer than blue lines in Figure 10c). A typical example is given in Figure 12. Two more examples can be found in Figures S2 and S7. It seems that in thunderstorms with frequent downward +IC flashes, normal IC flashes also tend to start at an altitude closer to the upper positive charge region. In other words, as the upper positive charge region is lifted by strong updrafts, initiation locations of IC flashes are also lifted, even though the main negative charge region remains unchanged. On the other hand, we did not notice any special characteristics of −CG flashes in thunderstorms with frequent downward +IC flashes, probably because the production of −CG flashes is not closely related with the upper positive charge region.

4. Discussion

4.1. Relationship Between Charge Layer Altitude and IC Flash Morphology

Proctor (1997) compared lightning flashes with low origins (1 to 7.4 km) and those with high origins (7.4 to 12 km) and found that channel extension speed was generally lower for high origin flashes. Wu et al. (2015) analyzed initial negative leaders in 662 IC flashes and demonstrated that the upward speed of initial negative leaders decreased as the initiation altitude increased. These results made us speculate that, if the initiation altitude is high enough, the initial negative leader of IC flashes would not even develop upward, and results of the current study confirm this speculation. Combining the results of previous studies and the current study, we have a complete picture of IC flashes in which characteristics of IC flashes gradually change as the initiation altitude increases, and we suspect that the increase of the initiation altitude is a direct result of the elevation of the upper positive charge region as illustrated in Figure 13 and described in the following paragraphs.

In relatively weak thunderstorms, IC flashes are usually dominated by an upward negative leader. The positive leader usually propagates horizontally (scenario A in Figure 13) or has a slightly downward movement (scenario B in Figure 13). The IC flash in Figure 3 of Rison et al. (1999) and the example in Figure S1 are typical examples. In fact, we believe that most normal-polarity IC flashes reported in the literature belong to these two types. In relatively strong thunderstorms, the upper positive charge region is lifted to higher altitudes due to strong updrafts, and initiation altitudes of IC flashes also increase. IC flashes initiated at relatively high altitudes tend to be dominated by downward positive leaders. Usually upward negative leaders still exist, but the upward speed is relatively low (scenario C in Figure 13). The flash in Figure 12 is a typical example; the speed of the upward negative leader was only about 1.9×10^4 m/s. Occasionally, downward +IC flashes as reported in this paper are produced. They are likely initiated from the upper positive charge region. In downward +IC flashes, negative leaders no long

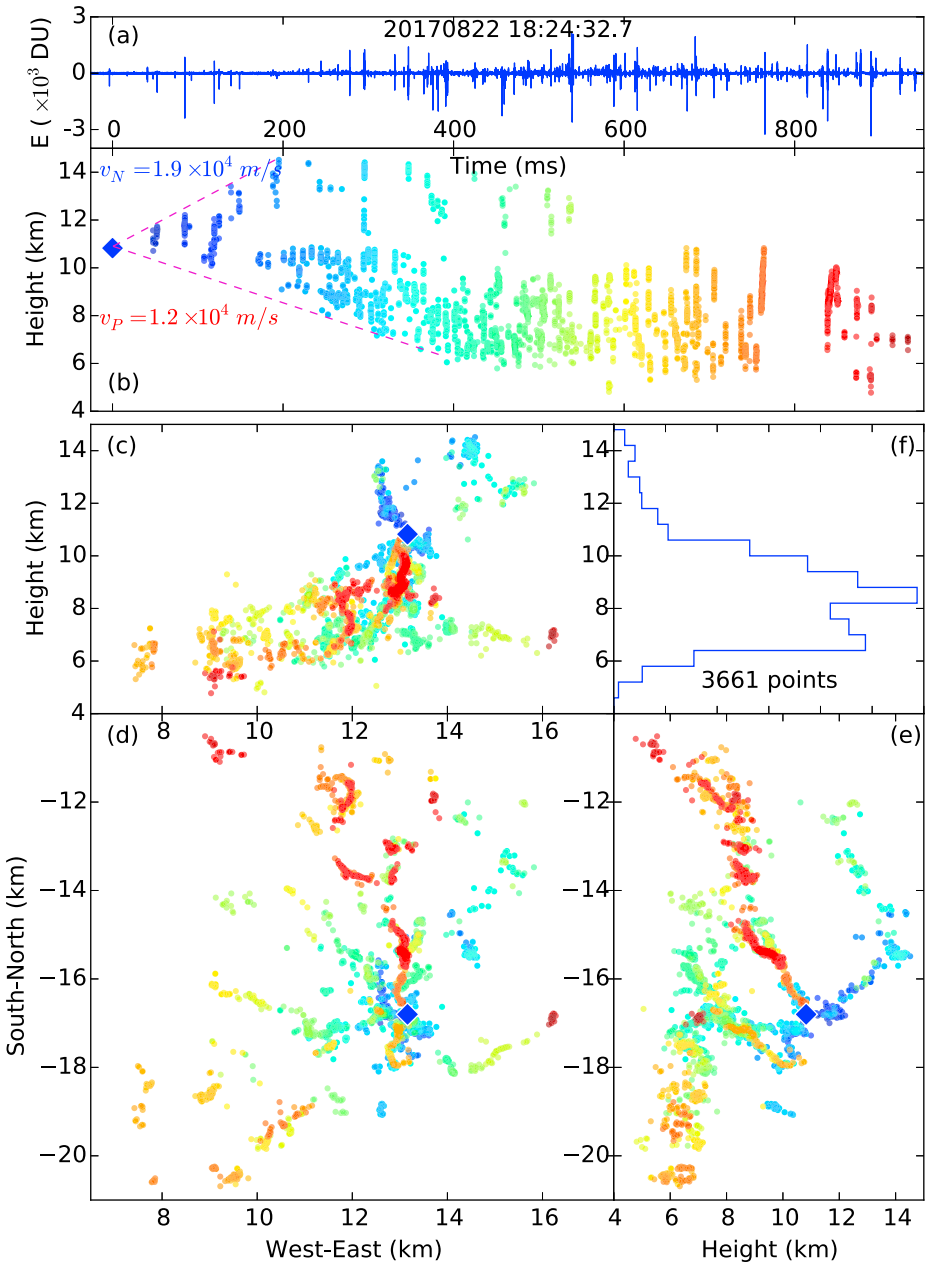

Figure 12. Location results of an intracloud flash starting with both upward negative leaders and downward positive leaders. Subplots are arranged as in Figure 2. The diamond represents the first located source of the flash.

travel upward; they usually move horizontally for a short distance with a low speed (scenario D in Figure 13).

It is important to note that in the illustration of Figure 13, while the upper positive charge region is lifted due to strong updrafts, the main negative charge region generally remains at the same altitude. This is based on the results of the present study and is also consistent with previous observations (Byrne et al., 1983; Krehbiel et al., 1984).

We also speculate that the upper positive charge region has a relatively small horizontal extent when downward +IC flashes are produced (scenario D in Figure 13). This is based on the observation that negative leaders (propagate in positive charge regions) in downward +IC flashes propagate for short distances. It can

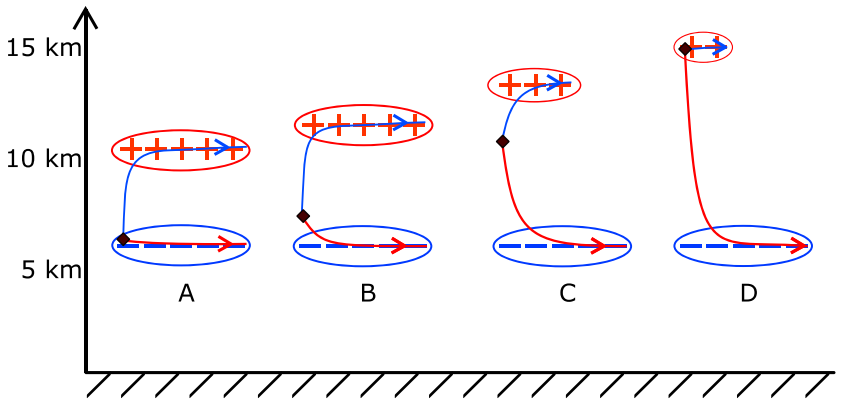

Figure 13. Illustration of different structures of intracloud flashes with different altitudes of the upper positive charge region. Blue curves represent negative leaders. Red curves represent positive leaders. Diamond signs represent initiation points.

also be inferred from Figure 5 that downward +IC flashes are likely associated with particularly strong updrafts in a narrow region, which may result in a lifted upper positive charge region with a limited horizontal extent.

The illustration in Figure 13 also has limitations. First, the thickness of charge layers is not considered in Figure 13. It is possible that the upper positive charge region may extend downward or the main negative charge region may extend upward. Second, Figure 13 only shows charge regions that are responsible for the detected lightning flashes; other charge regions such as the screening charge layer and the lower positive charge region may also exist. The evidence that the upper positive charge region is relatively small in scenario D is also not conclusive.

4.2. Remaining Questions

As this is the first study of the downward +IC flash, there are still many questions remaining to be answered. We will put forward three questions to which we currently do not have clear answers.

1. *Why do IC flashes rarely initiate near the main negative charge region when downward +IC flashes occur?* From Figure 10c, it seems that most IC flashes are initiated closer to the upper positive charge region. This implies that as the upper positive charge region is elevated, initiation locations of IC flashes are also brought upward. The main negative charge region remains at the same altitude, and −CG flashes occur as normal. It is an unexpected result that IC flashes are no longer initiated near the main negative charge region.
2. *Does the net charge of positive and negative leaders in the downward +IC flash equal to zero?* A basic assumption in modeling lightning channels is the overall neutrality, that is, positive and negative leaders originating from the neutral point carry equal amount of charges with opposite polarities (e.g., Kasemir, 1960; Riousset et al., 2007). According to examples of downward +IC flashes described in this paper, it seems obvious that positive leaders usually propagate for much larger distances and have many more branches than negative leaders. If we apply a simple electrostatic model assuming a stationary neutral point such as that described by Tran and Rakov (2017), we would get the result that the charge density in negative leader channels are many times larger than that in positive leader channels and keeps increasing as the flash develops.
3. *Do downward +IC flashes start with preliminary breakdown (PB)?* Although it has not been examined in detail, E-change pulses at the beginning of downward +IC flashes usually seem to be small, narrow, and sparse and are distinctly different from PB pulses reported in the literature (e.g., Ma, 2017; Marshall et al., 2014; Wu et al., 2013). (E-change waveforms of the three downward +IC flashes analyzed in section 3.1 are provided in Figures S9–S11.) This is in fact an expected result according to Wu et al. (2015), which showed that the PB of IC flashes initiating at higher altitudes generally produced less frequent PB pulses with smaller amplitudes and smaller pulse widths. Similar results have also been reported by Proctor (1997). If normal PB pulses are no longer detected, can we say that the lightning flash does not start

with PB? Or is it possible that the same physical process of PB still exists, but PB at high altitudes does not produce normal PB pulses?

5. Conclusions

In this paper, we reported a special type of IC flash called downward +IC flash. Downward +IC flashes are fundamentally different from normal IC flashes in that they do not contain upward initial negative leaders as found in normal IC flashes. Instead, they are dominated by downward positive leaders with speeds on the order of 10^4 m/s. Initial negative leaders still exist, but they only have horizontal propagations with speeds 1 order of magnitude smaller than normal negative stepped leaders, and they usually develop for a much smaller distance than initial positive leaders do.

Another important feature of downward +IC flashes is that they are usually initiated at higher altitudes than normal IC flashes. The majority of downward +IC flashes are initiated above 12 km, while most normal IC flashes reported in the literature are initiated below 10 km.

The charge structure responsible for downward +IC flashes is a positive dipole including a negative charge region at a normal altitude (near the −10 °C isotherm) and a positive charge region at a relatively high altitude (usually above the −50 °C isotherm), and downward +IC flashes are likely initiated from the upper positive charge region.

A short period in a thunderstorm producing a large number of downward +IC flashes is analyzed. When downward +IC flashes frequently occurred, −CG flashes occurred as normal and did not show any special characteristics. Other IC flashes, however, were somewhat special in that they were usually initiated at altitudes closer to the upper positive charge region and consisted of downward positive leaders more prominent than upward negative leaders.

The occurrence of downward +IC flashes is an expected result according to the finding of Wu et al. (2015) that the upward speed of initial negative leaders in IC flashes decreases as the initiation altitude increases. We further propose a possible relationship between the altitude of the upper positive charge region and the morphology of IC flashes illustrated in Figure 13. In relatively weak thunderstorms, IC flashes are usually initiated near the main negative charge region and are dominated by upward negative leaders. As the convective strength increases, the upper positive charge region is lifted to higher altitudes, and initiation altitudes of IC flashes also increase. In relatively strong thunderstorms, IC flashes are initiated near the upper positive charge region and are dominated by downward positive leaders.

Further studies based on a large sample of downward +IC flashes are needed. However, there are difficulties in conducting a statistical study. As can be seen in the three examples described in section 3.1, location results at the beginning of downward +IC flashes are usually not very good. This is due to the fact that E-change pulses at the beginning of downward +IC flashes are usually very small and sparse. As shown in Figures S9–S11, there were only a few pulses during the beginning 100 ms of the three downward +IC flashes; at many sites, these initial pulses were buried in the background noise and could hardly be recognized. This feature makes it very difficult to accurately locate the beginning part of downward +IC flashes. It is particularly difficult to accurately determine the initiation altitude, which is essential for a statistical study. We also speculate that the difficulty in locating downward +IC flashes is the reason that they have never been reported before.

Acknowledgments
This work was supported by the Ministry of Education, Culture, Sports, Science, and Technology of Japan (Grants 15H02597, 16H04315, and 18K13618). Location results of downward +IC flashes analyzed in this paper can be downloaded online (http://doi.org/10.5281/zenodo.1473170).

References

Behnke, S. A., Thomas, R. J., Krehbiel, P. R., & Rison, W. (2005). Initial leader velocities during intracloud lightning: Possible evidence for a runaway breakdown effect. *Journal of Geophysical Research*, *110*, D10207. https://doi.org/10.1029/2004JD005312

Byrne, G. J., Few, A. A., & Weber, M. E. (1983). Altitude, thickness and charge concentration of charged regions of four thunderstorms during trip 1981 based upon in situ balloon electric field measurements. *Geophysical Research Letters*, *10*(1), 39–42. https://doi.org/10.1029/GL010i001p00039

Caicedo, J. A., Uman, M. A., & Pilkey, J. T. (2018). Lightning evolution in two North Central Florida summer multicell storms and three winter/spring frontal storms. *Journal of Geophysical Research: Atmospheres*, *123*, 1155–1178. https://doi.org/10.1002/2017JD026536

Calhoun, K. M., MacGorman, D. R., Ziegler, C. L., & Biggerstaff, M. I. (2013). Evolution of lightning activity and storm charge relative to dual-Doppler analysis of a high-precipitation supercell storm. *Monthly Weather Review*, *141*(7), 2199–2223. https://doi.org/10.1175/MWR-D-12-00258.1

Fuchs, B. R., Bruning, E. C., Rutledge, S. A., Carey, L. D., Krehbiel, P. R., & Rison, W. (2016). Climatological analyses of LMA data with an open-source lightning flash-clustering algorithm. *Journal of Geophysical Research: Atmospheres*, *121*, 8625–8648. https://doi.org/10.1002/2015JD024663

Karunarathna, N., Marshall, T. C., Karunarathne, S., & Stolzenburg, M. (2017). Initiation locations of lightning flashes relative to radar reflectivity in four small Florida thunderstorms. *Journal of Geophysical Research: Atmospheres*, *122*, 6565–6591. https://doi.org/10.1002/2017JD026566

Kasemir, H. W. (1960). A contribution to the electrostatic theory of a lightning discharge. *Journal of Geophysical Research*, *65*(7), 1873–1878. https://doi.org/10.1029/JZ065i007p01873

Krehbiel, P. R., Tennis, R., Brook, M., Holmes, E. W., & Comes, R. (1984). A comparative study of the initial sequence of lightning in a small Florida thunderstorm. In *Proceedings of the Seventh International Conference on Atmospheric Electricity* (pp. 279–285). Albany, NY: American Meteorological Society.

Krider, E. P., Radda, G. J., & Noggle, R. C. (1975). Regular radiation field pulses produced by intracloud lightning discharges. *Journal of Geophysical Research*, *80*(27), 3801–3804. https://doi.org/10.1029/JC080i027p03801

Liu, C., Cecil, D. J., Zipser, E. J., Kronfeld, K., & Robertson, R. (2012). Relationships between lightning flash rates and radar reflectivity vertical structures in thunderstorms over the tropics and subtropics. *Journal of Geophysical Research*, *117*, D06212. https://doi.org/10.1029/2011JD017123

Lund, N. R., MacGorman, D. R., Schuur, T. J., Biggerstaff, M. I., & Rust, W. D. (2009). Relationships between lightning location and polarimetric radar signatures in a small mesoscale convective system. *Monthly Weather Review*, *137*(12), 4151–4170. https://doi.org/10.1175/2009MWR2860.1

Lyu, F., Cummer, S. A., Lu, G., Zhou, X., & Weinert, J. (2016). Imaging lightning intracloud initial stepped leaders by low-frequency interferometric lightning mapping array. *Geophysical Research Letters*, *43*, 5516–5523. https://doi.org/10.1002/2016GL069267

Ma, D. (2017). Characteristic pulse trains of preliminary breakdown in four isolated small thunderstorms. *Journal of Geophysical Research: Atmospheres*, *122*, 3361–3373. https://doi.org/10.1002/2016JD025899

MacGorman, D. R., Elliott, M. S., & DiGangi, E. (2017). Electrical discharges in the overshooting tops of thunderstorms. *Journal of Geophysical Research: Atmospheres*, *122*, 2929–2957. https://doi.org/10.1002/2016JD025933

Marshall, T., Schulz, W., Karunarathna, N., Karunarathne, S., Stolzenburg, M., Vergeiner, C., & Warner, T. (2014). On the percentage of lightning flashes that begin with initial breakdown pulses. *Journal of Geophysical Research: Atmospheres*, *119*, 445–460. https://doi.org/10.1002/2013JD020854

Mazur, V., & Ruhnke, L. H. (1993). Common physical processes in natural and artificially triggered lightning. *Journal of Geophysical Research*, *98*(D7), 12,913–12,930. https://doi.org/10.1029/93JD00626

Mecikalski, R. M., & Carey, L. D. (2017). Lightning characteristics relative to radar, altitude and temperature for a multicell, MCS and supercell over northern Alabama. *Atmospheric Research*, *191*, 128–140. https://doi.org/10.1016/j.atmosres.2017.03.001

Proctor, D. E. (1997). Lightning flashes with high origins. *Journal of Geophysical Research*, *102*(D2), 1693–1706. https://doi.org/10.1029/96JD02635

Rakov, V. A., & Uman, M. A. (2003). *Lightning: Physics and effects (ch. 9)*. UK: Cambridge University Press. https://doi.org/10.1017/CBO9781107340886

Riousset, J. A., Pasko, V. P., Krehbiel, P. R., Thomas, R. J., & Rison, W. (2007). Three-dimensional fractal modeling of intracloud lightning discharge in a New Mexico thunderstorm and comparison with lightning mapping observations. *Journal of Geophysical Research*, *112*, D15203. https://doi.org/10.1029/2006JD007621

Rison, W., Thomas, R. J., Krehbiel, P. R., Hamlin, T., & Harlin, J. (1999). A GPS-based three-dimensional lightning mapping system: Initial observations in central New Mexico. *Geophysical Research Letters*, *26*(23), 3573–3576. https://doi.org/10.1029/1999GL010856

Shao, X. M., & Krehbiel, P. R. (1996). The spatial and temporal development of intracloud lightning. *Journal of Geophysical Research*, *101*(D21), 26,641–26,668. https://doi.org/10.1029/96JD01803

Smith, D. A., Heavner, M. J., Jacobson, A. R., Shao, X. M., Massey, R. S., Sheldon, R. J., & Wiens, K. C. (2004). A method for determining intracloud lightning and ionospheric heights from VLF/LF electric field records. *Radio Science*, *39*, RS1010. https://doi.org/10.1029/2002RS002790

Stolzenburg, M., & Marshall, T. C. (2008). Charge structure and dynamics in thunderstorms. *Space Science Reviews*, *137*(1-4), 355–372. https://doi.org/10.1007/s11214-008-9338-z

Takahashi, T. (1978). Riming electrification as a charge generation mechanism in thunderstorms. *Journal of the Atmospheric Sciences*, *35*(8), 1536–1548. https://doi.org/10.1175/1520-0469(1978)035<1536:REAACG>2.0.CO;2

Tran, M. D., & Rakov, V. A. (2017). A study of the ground-attachment process in natural lightning with emphasis on its breakthrough phase. *Scientific Reports*, *7*, 15761. https://doi.org/10.1038/s41598-017-14842-7

Ushio, T., Heckman, S. J., Boccippio, D. J., Christian, H. J., & Kawasaki, Z. I. (2001). A survey of thunderstorm flash rates compared to cloud top height using TRMM satellite data. *Journal of Geophysical Research*, *106*(D20), 24,089–24,095. https://doi.org/10.1029/2001JD900233

van der Velde, O. A., & Montanyà, J. (2013). Asymmetries in bidirectional leader development of lightning flashes. *Journal of Geophysical Research: Atmospheres*, *118*, 13,504–13,519. https://doi.org/10.1002/2013JD020257

Villanueva, Y., Rakov, V. A., Uman, M. A., & Brook, M. (1994). Microsecond-scale electric field pulses in cloud lightning discharges. *Journal of Geophysical Research*, *99*(D7), 14,353–14,360. https://doi.org/10.1029/94JD01121

Weidman, C. D., & Krider, E. P. (1979). The radiation field wave forms produced by intracloud lightning discharge processes. *Journal of Geophysical Research*, *84*(C6), 3159–3164. https://doi.org/10.1029/JC084iC06p03159

Wu, T., Dong, W., Zhang, Y., Funaki, T., Yoshida, S., Morimoto, T., et al. (2012). Discharge height of lightning narrow bipolar events. *Journal of Geophysical Research*, *117*, D05119. https://doi.org/10.1029/2011JD017054

Wu, T., Takayanagi, Y., Funaki, T., Yoshida, S., Ushio, T., Kawasaki, Z.-I., et al. (2013). Preliminary breakdown pulses of cloud-to-ground lightning in winter thunderstorms in Japan. *Journal of Atmospheric and Solar-Terrestrial Physics*, *102*, 91–98. https://doi.org/10.1016/j.jastp.2013.05.014

Wu, T., Wang, D., & Takagi, N. (2018). Lightning mapping with an array of fast antennas. *Geophysical Research Letters*, *45*(8), 3698–3705. https://doi.org/10.1002/2018GL077628

Wu, T., Yoshida, S., Akiyama, Y., Stock, M., Ushio, T., & Kawasaki, Z. (2015). Preliminary breakdown of intracloud lightning: Initiation altitude, propagation speed, pulse train characteristics, and step length estimation. *Journal of Geophysical Research: Atmospheres*, *120*, 9071–9086. https://doi.org/10.1002/2015JD023546

Yoshida, S., Wu, T., Ushio, T., Kusunoki, K., & Nakamura, Y. (2014). Initial results of LF sensor network for lightning observation and characteristics of lightning emission in LF band. *Journal of Geophysical Research: Atmospheres*, *119*, 12,034–12,051. https://doi.org/10.1002/2014JD022065